



ISTITUTO NAZIONALE DI RICERCA METROLOGICA Repository Istituzionale

Rock temperature variability in high-altitude rockfall-prone areas

This is the author's submitted version of the contribution published as:

Original

Rock temperature variability in high-altitude rockfall-prone areas / Nigrelli, Guido; Chiarle, Marta; Merlone, Andrea; Coppa, Graziano; Musacchio, Chiara. - In: JOURNAL OF MOUNTAIN SCIENCE. - ISSN 1672-6316. - 19:3(2022), pp. 798-811. [10.1007/s11629-021-7073-z]

Availability:

This version is available at: 11696/73970 since: 2022-06-13T15:30:18Z

Publisher:

Springer

Published

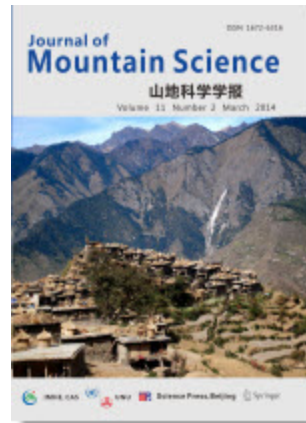
DOI:10.1007/s11629-021-7073-z

Terms of use:

This article is made available under terms and conditions as specified in the corresponding bibliographic description in the repository

Publisher copyright

(Article begins on next page)



Rock temperature variability as a driving factor of rockfalls

| | |
|------------------|--|
| Journal: | <i>Journal of Mountain Science</i> |
| Manuscript ID | 21-7073 |
| Manuscript Type: | Original Article |
| Keywords: | Rock temperature, Rockfalls, European Alps |
| Speciality: | rock temperature |
| | |

SCHOLARONE™
Manuscripts

Rock temperature variability as a driving factor of rockfalls

Abstract

In a context of cryosphere degradation caused by climate warming, rock temperature is one of the main driving factors of rockfalls that occur on high-elevation mountain slopes. In order to improve the knowledge on this critical relationship, it is necessary to: i) increase measurement capability for rock temperature and its variability in different lithological and slope/aspect conditions; ii) increase local scale studies; iii) increase the quality and the comparability of the observational data. This paper shows an example of metrological characterization of sensors used for rock temperature measurement in mountain regions aiming at establishing. Metrological traceability and evaluating measurement uncertainty. Under such approach, data and results from temperature measurements carried out in the Bessanese high-elevation experimental site (Western European Alps) are illustrated. The here adopted procedures for the calibration and field characterization of sensors allow to measure temperature in different locations, depths and lithotypes within 0.098 °C of overall uncertainty. The main results are: i) Metrological traceability is fundamental to assess data quality and establish comparability among different measurements; ii) There are strong differences between air temperature and near-surface rock temperature; iii) There are significant differences of rock temperature acquired in different aspect conditions. Solar radiation, slope/aspect conditions and lithotype, seem to be the main driving factors of rock temperature.

1. Introduction

In a context of a climate warming that affects the mountain cryosphere, landscapes are evolving and new hazards are emerging. Changes in mean and extreme air temperature and precipitation values are important conditioning and triggering factors for many natural instability processes that occur in the mountain cryosphere (Allen et al. 2017). During the last 30 years, one of the most relevant impacts of climate change in the European Alps (hereinafter Alps) has been the increase of natural instability processes that occurred on high-elevation mountain slopes (Fischer et al. 2012a; Allen et al. 2013). In particular, a growing number of rockfalls has been observed and documented (Ravelle et al. 2017; Paranunzio et al. 2019a; Paranunzio et al. 2019b; Chiarle et al. 2021; Guerini et al. 2021; Nigrelli et al. 2021b). This trend is due to the cryosphere (including permafrost) degradation caused by global warming (Harris et al. 2009; Hock et al. 2019). Air and rock temperature increase, seems to be the most relevant driving factors of rockfalls that occur on high-elevation mountain slopes (Chiarle et al. 2015; Nigrelli et al. 2018). From a thermodynamic point of view, a complete modelling and understanding of heat transfer processes and associated temperature values and gradients in rocks exposed to radiative, convective, conductive and condensation forcing is highly complex. At the air-rock interface there are thermal exchanges by irradiation, convection, condensation and evaporation, while inside the solid rock thermal exchanges occur only by conduction. Moreover, the thermal regime of the rock surface is very complex because is highly dependent on short- and longwave radiation, albedo, surface roughness, snow and vegetation cover and its distribution/variability in time and space (Haberkmorn et al. 2015). Currently, there are no data loggers capable of measuring and storing the temperature data acquired at the air-rock interface for long periods of time (more than one year) and with high resolution, sensitivity and accuracy. Despite temperature data at the air-rock interface is fundamental, at present it is not possible to acquire this data with a level of accuracy fit for the purposes of improving knowledge on instability and rockfalls. In order to better understand the effect of climate change to slope instability, in a context of cryosphere degradation, it is necessary to acquire data on rock temperature (in particular rock-face temperature), data on its variability and on its relation with the main geomorphological and meteorological parameters. This investigation process is not easy because:

- i) Long time series of rock temperature data, acquired in the mountain cryosphere of the Alps are rare;
- ii) Where available, rock temperature data are often acquired by means of sensors and acquisition chains with unknown measurement uncertainty and undocumented instrument traceability;
- iii) The weather stations located in the mountain cryosphere of the Alps (specifically above 2500 m a.s.l.) are few.

Despite these difficulties, during the last 20 years several studies on rock temperature have been carried out in the Alps, with interesting results (Gruber et al. 2004; Hasler et al. 2011; Moor et al. 2011; Magnin et al. 2017; Weber et al. 2017; Viani et al. 2020). These studies highlight the importance of local studies, carried out on high-elevation experimental sites. The local scale approach through the availability of instrumented experimental areas allows to obtain very useful results in terms of relations between climate variability and thermal conditions of geological materials, responsible of the development of slope instability in the cryolithosphere (van Everdingen 1998). However, to obtain more accurate results, two fundamental aspects need to be considered: a constant check of data quality and the standardization of measurement techniques, to improve comparability in time and space. These

1
2
3 aspects are highlighted in the Handbook on Periglacial Field Methods, edited by the International Permafrost
4 Association (Hummlun et al. 2004). However, this handbook does not yet report the need of knowing the
5 measurements uncertainty and the instruments traceability. Furthermore, the works that have been published in
6 recent years still do not follow agreed standard approaches and common practices in rock temperature measurement
7 methods. In summary, the key questions related to this research field are the following:

- 8 i) How is it possible to increase rock temperature knowledge in the mountain cryosphere?
- 9 ii) How is it possible to increase the quality and the comparability of the temperature data?

10 On such basis, the aims of this work are three:

- 11 i) To propose a measurement method which includes a robust metrological approach delivering measurement
12 uncertainty evaluation and improved data quality through documented traceability and comparability;
- 13 ii) To apply the proposed measurement approach to a high-elevation experimental site, in order to quantify rock
14 temperature, its variability and its relation with the main geomorphological and meteorological parameters;
- 15 iii) To promote through the international scientific community the need for shared and standardized procedures,
16 and the importance of local scale studies through the realization of instrumented experimental areas in the
17 mountain cryosphere.

18 In this study, we report results coming from our high-elevation experimental site, during two years of measurements
19 in the framework of the RiST2 Project.

20 **2. Study area and measurement design**

21 The temperature monitoring site (TMS) considered for this study is located in the Bessanese high-elevation
22 experimental basin in the North Western Italian Alps (Lat. 45.2979 °N, Long. 7.1433 °E, Figure 1). The main
23 features of this experimental site are described in detail in Viani et al. (2020). The lithotype of the TMS is an
24 outcrop of calc-schists. In this site, three rock-faces with different orientation (N-E, S-E, S-W) were individuated
25 (respectively TMS1, TMS2 and TMS3). In each of these sites, three instruments for temperature measurement and
26 recording (sensors with embedded data loggers) were inserted in the rock, perpendicularly to the surface,
27 respectively at a depth of 10 cm (also identified as near-surface rock temperature, NSRT), 30 cm and 50 cm (Table
28 1).

29 In this experimental configuration the N-W exposure is missing due to the geological and topographical conditions
30 of the site. This TMS is ideal to carry out continuous monitoring in the calc-schists, a predominant lithotype in the
31 western alpine sector.

32 Air temperature and others meteorological data were provided by an automatic weather station installed by ARPA
33 Piemonte in 1988. The AWS is located at about 130 m from the TMS and its sensors are positioned 6 m above the
34 ground level. Since 2018, the AWS also acquires total incident and reflected solar radiation (Nigrelli et al. 2021a).

35 **3. Measurement approach**

36 The methodology we propose here consists in an innovative approach integrated by the use of advanced
37 technologies. The main novelty of our approach is the goal to achieve a fully documented measurement traceability.
38 This is obtained in two specific steps:

- 39 i) Selection of high quality instruments and sensors, considering the condition of use, the possibility to store
40 data for long periods, the possibility to be calibrated several times;
- 41 ii) Definition of specific calibration methodologies and procedures; sensors calibration with associated
42 calibration curve and uncertainty, including characterization of the field use to also evaluate further
43 components of the overall measurement uncertainty (not limited to the calibration uncertainty);

44 In cryosphere studies, a fully documented metrological traceability of measurements is frequently missing but it is
45 fundamental for data comparability in space and in time (Merlone et al. 2015).

46 For this study, we used MadgeTech MicroTemp Data Loggers (MT). This choice was made because MTs are
47 miniaturized (length 66 mm, diameter 18 mm, weight 14 g), waterproof, self-contained temperature data loggers that
48 can be easily inserted into rock and other geological materials such as coarse and fine debris, soil, ice, water. They
49 can measure and store data for more than one year, since they have user-replaceable batteries, and work in the
50 temperature range [-40; +80] °C, with a resolution of 0.1 °C. Differently from other disposable sensors, MTs can be
51 routinely calibrated, their measurements traceable to SI standards. Based on our experience, these MTs offer an
52 excellent compromise between ease of use in extreme conditions, cost and data quality.

53 The proposed measurement approach consists in the following four steps:

54 Step 1. Laboratory calibration of the MTs.

55 This calibration is necessary to: a) establish full traceability, b) correct for instrumental errors, c) determine the
56 calibration uncertainty, a key component of the overall measurement uncertainty, before and after the on-site

deployment. The calibrations have been performed at the Italian National Metrology Institute (Istituto Nazionale di Ricerca Metrologica, INRiM), by comparison against a reference standard thermometer traceable to national reference fixed points. The calibration was performed by comparison in a characterized liquid bath, in the range [-20; 40] °C, a Fluka 1594A was used for reading the reference PT100 thermometer. The calibration uncertainty before data acquisitions was evaluated taking into account all components such as the MT resolution, the bath stability and uniformity and the reference thermometer uncertainty.

All procedures here adopted are in agreement with the GUM, Guide to the expression of uncertainty in measurement, JCGM 100:2008, while the terminology here used is aligned with the VIM, International Vocabulary of Metrology, JCGM 200:2012).

Step 2. Evaluation of measurement uncertainty.

The measurement procedure here adopted, which minimizes the difference from the calibration conditions, including the tests, characterization and calibration results, a tentative measurement uncertainty budget was evaluated. The overall measurement uncertainty, excluding drift and shocks, accounts to 0.098 °C which is rounded to 0.1 °C, also according to the instrument resolution, which becomes a correct and evaluated indicator of the measurement uncertainty (Table 2). Through this approach and further statistical analysis, it is possible to obtain traceable temperature data with uncertainties of some 0.01 °C while, in general, in the environmental research field data is normally declared at 0.1 °C with rarely complete traceability documentation.

Step 3. Rock temperature monitoring.

Considering that the bibliographic analysis did not point out clear standardized practices in relation to depth configurations, we chose to position the MTs at three different depths in the rock (10, 30 and 50 cm, Table 1). The MTs have been preventively smeared with white silicon grease to maximize the contact with the rock, thus improving the thermal conductivity (Figure 2). This is also the condition met in liquid bath during calibration, thus making the calibration curve and associated uncertainty more representative of the measurement conditions. Data acquisitions of the nine MTs started on 20 July 2018 and ended on 5 August 2020, without missing data. Rock temperatures were logged every 30 minutes: MTs acquisitions were synchronized with the AWS acquisitions, in order to make a correct time comparison. Hours are expressed in UTC+2 (CEST).

Step 4. Data analysis.

The local scale variability of rock temperature and their relation with the main geomorphological and meteorological parameters were processed and plotted. The on-site daily maximum temperature gradient (or lapse rate, DTLR) of calc-schist rock was also calculated. For our analyses, we considered the maximum daily temperature, because this is one of the main driving factors of rockfalls that occur at high-elevation. The DTLR is an important parameter that is used for the calculation of the thermal conductivity of materials, through the application of Fourier's law (Schön et al. 2015). The formula applied to calculate DTLR is: $\Delta T/\Delta x$ (°C/cm), where ΔT is the difference of daily maximum temperature acquired by two MTs and Δx is the difference between two depths, in our cases is set to 20 cm. The zero-curtain periods, which indicate the thermal insulation caused by the snow cover, were determined for days with near-surface rock temperature between [-0.2; +0.2] °C, a range similar to that applied in Gubler et al. (2011). The zero-curtain periods were not included in the calculation of DTLR. Furthermore, the main physical properties of the calc-schists were determined. Color, bulk density and specific heat capacity were determined in laboratory on rock samples of about 10-15 cm³ of volume, collected close to each temperature monitoring site.

Rock color was determined both in wet and dry conditions, by using the Munsell Rock Color Chart. Density (ρ) is defined as the quotient of mass “*m*” (sample of about 5 g) and volume “*V*” of a material ($\rho = m/V$). In this work, the bulk density was calculated, i.e. the mean density of the considered rock volume, including pores. Bulk density (g/cm³) was calculated by means of pycnometers (Schön et al. 2015). Finally, the specific heat capacity (c_p) is defined as the ratio of the heat input “*Q*” to the product of the mass “*m*” (sample of about 50 g) and the resulting temperature increase “ ΔT ”, where the subscript “*p*” indicates specific heat capacity at constant pressure: $c_p = Q/(m*\Delta T)$. The specific heat capacity (in J/kg K) was calculated by using a Dewar vessel calorimeter (Schön et al. 2015). Temperature in the calorimeter was measured by using a copper-constantan thermocouple (measurement accuracy 0.2 %) and it was recorded each 1 s by means of a data logger.

4. Results

Table 3 synthesizes rock and air temperature acquired for the entire period of measurement. Regarding rock temperatures, the highest value was recorded by the MT Q62110 (TMS3, 10 cm depth): 40.8 °C at 18:00 hours of the 28/06/2019 with nearby air temperature of 18.5 °C, and difference between rock and air temperature of 22.3 °C. The lowest value was recorded by the MT Q61213 (TMS1, 10 cm depth): -7.5 °C from 3:00 hours to 4:30 hours of the 14/11/2019 (air temperature -10.3 °C, ΔT between rock and air temperature -2.8 °C). Regarding air

temperatures, the highest value observed is 19.9 °C (16:00 hours of the 25/06/2019) and the lowest value is -18,8 °C (6:30 hours of the 26/03/2020).

Figure 3 shows rock and air temperature and snow depth trends during the entire observed period. The trends observed for rock temperature are similar, but several differences in the quantitative values have been found in relation to the different depths of data loggers and to the different aspect of the three measuring site. In this figure, particular evident is the zero-curtain period. The zero-curtain state is characterized by a constant temperature close to 0 °C due to the snow cover (thermal insulation) and due to the latent heat released in the melting snow pack (Hasler et al. 2011; Kellerer-Pirklbauer 2017; Viani et al. 2020). This figure also highlights the limited number of diurnal freeze-thaw cycles in the rock: in fact, when the rock is out of the zero-curtain, air temperature tends to remain above 0 °C.

Figure 4 shows an example of rock and air temperature trends in TMS3, during four consecutive days (from 1 to 4 September 2019) and their relation with the global and reflected solar radiation. In this figure it is important to observe the time shift among the peak values of all the considered parameters.

In Figure 5 the descriptive statistics of the two DTLRs calculated for each TMS, using the three different depths (10 cm vs 30 cm and 30 cm vs 50 cm) are reported. In the TMS1 the mean DTLRs are 0.18 °C/cm (± 0.11 °C/cm; $n = 262$) and 0.08 °C/cm (± 0.06 °C/cm; $n = 262$) respectively for 10 cm vs 30 cm and 30 cm vs 50 cm. In the TMS2 the mean DTLRs are 0.25 °C/cm (± 0.18 °C/cm; $n = 365$) and 0.06 °C/cm (± 0.06 °C/cm; $n = 365$) respectively for 10 cm vs 30 cm and 30 cm vs 50 cm. In the TMS3 the mean DTLRs are 0.39 °C/cm (± 0.28 °C/cm; $n = 391$) and 0.09 °C/cm (± 0.10 °C/cm; $n = 391$) respectively for 10 cm vs 30 cm and 30 cm vs 50 cm. For this parameter, the linear correlation of the two DTLRs for each TMS was also calculated. In TMS1 the linear correlation between the two DTLRs is: $y = 0,5022x - 0,0121$ ($R^2 = 0,83$); in TMS2 the linear correlation is: $y = 0,3021x - 0,0188$ ($R^2 = 0,86$); in TMS3 the linear correlation is: $y = 0,3205x - 0,0305$ ($R^2 = 0,88$).

5. Discussion

The work here presented is based on a novel and robust methodology that involves improved understanding of the whole measurement process: from the sensor calibration and characterization, to the measurement procedure and complete uncertainty analysis. This process allowed more robust understanding on the local scale relationships among rock temperature, geomorphological features and meteorological parameters through a spatio-temporal comparability of data. In this discussion particular relevance is given to the rock temperature variability as a driving factor of rockfalls. In relation to the results obtained, the main key results are as follows:

- i) Metrological traceability is fundamental in data acquisition to achieve comparability and to accurately capture trends;
- ii) Strong differences exist between air and rock temperature, in particular NSRT;
- iii) Significant differences exist between temperatures acquired in each measurement site (TMS1, TMS2 and TMS3), with particular reference to NSRT;
- iv) DTLR shows a very marked variability between temperatures acquired in each measurement site (TMS1, TMS2 and TMS3), especially between the shallower MTs;
- v) Long periods of zero-curtain;
- vi) Only a few freeze-thaw cycles occur in the NSRT, with respect to the air temperature.

Point i). Metrological traceability of measurements is a fundamental requirement to achieve data comparability and a fundamental aspect to accurately capture trends. Improved and dedicated calibration procedures, uncertainty evaluation of field measurements results is being carried out under a direct collaboration between metrologists and scientists operating in instrumented experimental areas in the cryosphere. Field measurements of temperature is a key investigation for cryosphere studies, in high mountain regions and Arctic environments. Among the numerous Essential Climate Variables (ECVs), defined by the Global Climate Observing System (GCOS) terrestrial recommended measurements include quantities of interest in cryosphere studies also under a co-siting vision with the proposal of a Global Climate Reference Network (Thorne et al. 2018). The WMO's Global Cryosphere Watch (GCW) has deep interest in implementing metrology and metrological approach. Result of interest for GCW have already been delivered by European Metrology Research Programme Joint Research Projects such as MeteoMet (Merlone et al. 2012; Merlone et al. 2015). The activities on improving the data quality for permafrost measurements, the discussion opened by the series of "Arctic Metrology workshops", the calibration campaign in high mountain regions and the proposal for a dedicated metrology infrastructure for polar research are all valuable examples. Such direct collaboration with the metrology community brings proved benefit and progresses in the quality of data recorded by the multitude of network and stations of GCW and more in general on studies on the cryosphere.

1
2
3 It is under such framework, that the work here presented addresses the needs of the GCW as an example of
4 documented traceability and best practice for calibration and measurement uncertainty.
5

6 Point ii). Strong differences between air temperature and NSRT (MT at 10 cm depth). These differences are visible
7 in Figure 3. During Summer, the minimum daily air temperatures is above 0 °C for a several consecutive days,
8 causing ice melting at a growing depth in rock slopes, and consequent permafrost degradation. In the night-time the
9 rocks cool down and, the following morning, before sunrise, the NSRT is sometimes higher than the air temperature
10 of a few degrees, due to the thermal inertia of the rock mass with respect to air re-warming. An example of this
11 process is shown in Figure 4. During sunny days, high values of ΔT between air and rock temperature were found
12 (Figure 4, 3 and 4 September 2019). When direct solar radiation is absent, e. g. during cloudy days (1 and 2
13 September 2019), differences are minor but still significant. The NSRT is higher than air temperature, due to major
14 radiation absorption, transferred into available heat content, here detected as temperature increase. Even if ΔT
15 between air and rock decreases with increasing rock depth (see Figure 4), it never becomes zero. These differences
16 have been reported in some papers that compared air temperature with NSRT, such as in Haberkorn et al. (2016),
17 Viani et al. (2020). Our study confirms that there is a low linear correlation between daily maximum air temperature
18 and daily maximum NSRT (zero-curtain days excluded, see point v). Linear correlation coefficient (R^2) for the three
19 pairwise comparisons are 0.37 (with 262 days), 0.52 (365 days) and 0.46 (391 days), respectively for TMS1, TMS2
20 and TMS3. These results must be taken into serious consideration when analyzing the thermal conditions associated
21 with the triggering of slope instability. In fact, simply taking into account air temperature trend can lead to a
22 significant underestimation of rock mass temperature, during the summer or even all year round, in case of vertical
23 rock walls where snow cannot accumulate.

24 Point iii). Significant differences between temperatures acquired in each measurement site (TMS1, TMS2 and
25 TMS3). These differences are clearly visible in Figures 3 and are particularly marked for NSRTs. NSRT is mainly
26 influenced by rock-face slope/aspect and by the thermal characteristics of the specific lithotype, as found also by
27 other authors (Gruber et al., 2004; Matsuoka 2008; Fischer et al., 2012b; Viani et al. 2020). Differences in solar
28 radiation and in the timing and depth of the snow cover are also important (Haberkorn et al. 2015; Haberkorn et al.
29 2016). Data in Table 3 highlight this point, in particular MT Q62110 in TMS3. This MT is inserted in a rock-face
30 that is oriented 225 °N, with a slope angle of 45°. This optimal positioning, in relation to the absorption of solar
31 radiation, is evident in the curve of temperature growth in Figure 4. In this figure, after sunrise, temperature acquired
32 by MT Q62110 (10 cm depth), rises rapidly, well above that of the air, and also while this latter remains almost
33 stable, until the angle of incidence of the sun decreases. The same trend is displayed by the other MTs in rock, with
34 different timing and absolute values, in relation to the different slope/aspect conditions of the rock-face.
35 In Figure 4 is clearly visible the time shift between the maximum values of all the parameters reported. This time
36 shift is specific to each lithotype because it depends on the thermal properties of each rock, in relation to daily solar
37 radiation increases/decreases.

38 Point iv). The data relating to the thermal gradient (or lapse rate) of the rocks, provide one of the most important
39 parameters useful to the definition of the heat transfer models in rock. Due to the different physical, chemical and
40 mineralogical characteristics of the different types of rocks, these data must be acquired for each lithotype. As
41 reported above, the lithotype of the three TMSs is an outcrop of calc-schist and the DTLRs of this lithotype are
42 summarized in Figures 5. In this figure, differences in the DTLR values are clearly visible. The most evident
43 differences are observed in the calculated values for TMS1-a (0.18 °C/cm), TMS2-a (0.25 °C/cm) and TMS3-a
44 (0.39 °C/cm). These values indicate that a compact calc-schist rock exposed to SE heats up twice as much as the
45 same rock exposed to the NE. Very evident differences are also observed for the extreme values (the whiskers of the
46 box plot). The results of our study confirm that daily temperature fluctuations are less pronounced for rock faces
47 exposed towards N, than for those exposed towards S, reaching the highest values for SW exposures. As a result,
48 south-facing rock slopes are particularly exposed to cycles of thermal expansion/contraction, even if temperature
49 remains above 0°C (Collins and Stock 2016), which can cause the progressive degradation of rock properties. On
50 this regard, Nagai et al. (2013), for example, found that southwest-facing slopes supply the largest quantity of debris
51 mantle on glaciers in the Bhutan Himalaya. On the contrary, North-facing slopes are more sensitive to seasonal
52 temperature fluctuations and in general to climate warming, since their temperature depends on air temperature more
53 than on solar radiation, as it happens for South-facing slopes. In fact, North-facing slopes are the source of many
54 rock falls occurred in recent decades (Viani et al., 2020).

55 The values calculated for TMS1-b (0.08 °C/cm), TMS2-b (0.06 °C/cm) and TMS3-b (0.09 °C/cm), are substantially
56 the same.
57
58
59

Furthermore, the thermal diffusivity coming from the surface is not transmitted in depth, and its effect can be estimated almost nil at a depth close to one meter. The thermal diffusivity is a measure of penetration of temperature changes into a material (Schön et al. 2015). According to these results, we can figure out that in compact calc-schist rocks, with a specific heat capacity of 818 J/kg K, rock temperature variability plays an important role as a driving factor of rockfalls in the most superficial layer. A different and stronger effect linked to thermal diffusivity occurs in fractured rocks where, within these fractures, there is the presence of air, water or ice. However, it should not be forgotten that rocks are strongly anisotropic. In relation to this, several on-site measurement points and several years of measurements are required, as also reported in Keller-Pirklbauer (2017). In the Cryosphere-Climate laboratory of the CNR-IRPI of Torino, the determination of the thermal properties of the different types of rock that are predominant in the Alps is underway, in order to develop accurate and exportable heat transfer models of rocks that can cause rockfalls in the Alps.

Point v). The entire time-series of measurements highlights the impact of snow cover on rock temperature (Figure 3). The thermal insulation properties of snow are well known (Barry, 2008; Harris et al., 2009; Barry, 2011; Mingko, 2012). This is the so-called zero-curtain effect. When data loggers are under snow cover, they are thermally insulated from the atmosphere and consequently their temperature is close to 0 °C, decoupling them from air temperature trend. This situation confirms the marked role of the snow cover, in our case from a thickness of about 15-20 cm, as also other authors reveal (Haberhorn et al., 2015). Since the height of the holes in the rock faces selected for this study are 100 cm and 130 cm, when the mean snow depth during winter and spring can be higher than 250 cm, and the slope range of the three TMSs is from 45° to 50°, TMSs are under the insulating effect of the snow from late autumn to late spring. This situation can be considered a negative aspect of this work, because it considerably reduces the number of useful measures.

Point vi). Field monitoring in the World has highlighted the roles of diurnal and annual frost cycles in controlling the timing and magnitude of frost weathering (Matsuoka et al. 2008). The weathering by freeze-thaw cycles is an important process that occur in the rock slopes of the Alps. However, in our study, only a few freeze-thaw cycles in rock were identified. The main causes are two: the first one is the relatively low altitude of the measurement site (<3000 m a.s.l.); the second one is the presence of snow cover for a long period each year. (from late Autumn to late Spring), precisely in the months in which the air temperature undergoes most of the oscillations above and below 0°C and could thus causes several freeze-thaw cycles and the so-called thermal stress weathering. These affect rock, debris, ice and water temperature (Fischer et al. 2012a; Fischer et al. 2012b; Weber et al. 2017). In these seasons, when snow cover is absent from near-vertical rock slopes, NSRT can be higher than near-surface air temperature and can be some degrees above 0 °C: this is due to strong short-wave solar radiation. Considered that near-vertical rock slopes are also the most prone to instability, and that some of the largest slope failures occurred in recent years in permafrost alpine areas happened from Autumn to Spring (Paranunzio et al. 2018; Paranunzio et al. 2019a), the knowledge of the actual thermal condition of rock slopes during these seasons is crucial for understanding processes leading to failure (Gruber et al., 2004; Weber et al. 2017). In order to solve this aspect, it would be necessary to set up a measuring site at a higher altitude than the current one, but this entails greater logistical difficulties.

Summing up we conclude that, in order of importance, solar radiation, slope/aspect conditions and lithotype, seem to be the main driving factors of rock temperature variation at short time-scales (daily to seasonal). It is important to underline that a more in-depth comparison between the results reported in this work and the results reported in the bibliography is difficult, due to the significant differences between the applied methodologies and the different sensor types used.

Regarding the crucial parameter of temperature, however, the reference datum is air temperature, as it is usually the only available. However, this study highlights the strong difference between air and rock temperature and the time shift that exists between their peak values. This means that, even with all the limitations/exceptions of the case, estimating the temperature of the rock on the basis of the air temperature alone can lead to a significant underestimation of rock temperature, and therefore to an incorrect interpretation of the mechanisms associated with geomorphological dynamics/slope instability. This could explain, e.g., rockfalls occurred at high altitudes in Winter, when air temperature is well below 0 °C, difficult to interpret if only air temperature is considered (Schnepfleitner et al. 2018). It is evident that solar radiation is critical in this regard, both in terms of cloudiness/seasonality, and with regard to slope and aspect of rock masses, as other authors mentioned above have also reported.

As already mentioned, the lithological composition of rock masses also plays a role in the thermal behavior of mountain slopes: new data acquisitions in the laboratory and in the field, specific for each lithotype involved in

rockfall are necessary. The methodological approach used for this work, ensuring comparability of results and definition of measure uncertainties, is the most appropriate to investigate also these aspects.

6. Conclusions

This paper shows one example of the application of procedures aimed at the metrological characterization of sensors used for the measurement of temperature in mountain cryosphere. The main novelty is a rigorous application of metrological principles to establish traceability and fully evaluate measurement uncertainty for this specific application and linked studies on cryosphere degradation. The case study in an instrumented experimental area, the Bessanese glacial basin, is the first field application. Data and results from two years of measurements have been reported. This case study can be considered a preliminary approach for new and more modern research methods regarding temperature studies in glacial and periglacial areas, with a focus on temperature as a driving factor of slope instability.

Answering the two key questions reported in the introduction, we conclude that:

i) How is it possible to increase rock temperature knowledge in the alpine cryosphere?

Rock temperature knowledge in the alpine cryosphere can be increased by extending and comparing the instrumented experimental areas; rock blocks and outcrops can be used as analogous of rock slopes, when these latter are difficult and/or dangerous to reach. This solution can be the right compromise to new data, while keeping low cost and risks associated with this type of investigation. These instrumented experimental areas could become authentic reference sites, in which to collect data, but also to develop new methodological approaches and to test and compare different and evolving instruments and technologies. Furthermore, rock temperature knowledge in the alpine cryosphere can be increased by using sensors and metrological approaches that take favor of a fully traceability of measurements.

ii) How is it possible to increase the quality and the comparability of the data?

It is possible to increase the quality of the data using local scale approaches, applying shared and standardized methodologies, using sensors and acquisition chains with known measurement uncertainty. In a long-term vision, setting up an experimental site designed according to the results of the analysis on top quality-reference grade measurements represents a preliminary example towards a network of reference sites at large regional or future global scale. During the last twenty years, several projects in the cryosphere have been implemented, several working groups have been activated, led by the most important government agencies or associations in the world, for example the Global Cryospheric Watch of the World Meteorological Organization (WMO-GCW), the National Snow and Ice Data Center (NSIDC), the International Permafrost Association (IPA), the International Association of Cryospheric Sciences (IACS). During these twenty years many instrumented experimental areas in the cryosphere have been equipped, following independent approaches and different solution. This results in a low level of data comparability, very different technical methods adopted, total absence of measurement guidelines or discussed dedicated calibration procedure. Full understanding and evaluation of measurement uncertainty is not present in literature, and rarely reported results include at least instrumental uncertainty evaluation. This situation is well known by WMO-GCW, which in 2020 formed specific working groups tasked to define standards and best practice for observations and measurements of parameters of the cryosphere: snow, permafrost and glaciers. The final goal is to extend the WMO guide No.8 to the cryospheric obserations. The approach here proposed can be intended as a local scale case study in order to stimulate the international scientific community towards the adoption of shared and standardized procedures. When general principles will be formally adopted, a reference network can originate in harmonized and comparable way, for generating long term measurement records.

Climate change is significantly modifying the cryosphere and one of the most evident consequences is the increase of natural instability processes, and of related hazards and risks. For improve knowledge on hazards and risks in the cryosphere, a rapid progress in such research activities is need. To achieve this, it is necessary to combine efforts by applying standardized methodologies, increasing data acquisition and sharing results within and among different communities.

Acknowledgements

The authors wish to thank: Ing. Renato Riva (PANOMAX Italia) for his expertise and his availability in setting up the visual monitoring of the study area; Ing. Secondo Barbero (ARPA Piemonte) for providing climatic and sensor data; Guido Rocci (Municipality of Balme) for the support given to the project and for the hospitality offered at the Les Montagnards hut; Roberto Chiosso and his staff for the support given to the project and for the hospitality offered at the Bartolomeo Gastaldi hut.

Funding Information

This work was carried out in the framework of the RiST2 Project, co-financed by Fondazione Cassa di Risparmio di Torino.

References

- Allen S, Frey H, Huggel C, et al. (2017) Assessment of Glacier and Permafrost Hazards in Mountain Regions – Technical Guidance Document. GAPHAZ, Zurich, Switzerland/Lima, Peru
- Allen S, Huggel C (2013) Extremely warm temperatures as a potential cause of recent high mountain rockfall. *Global and Planetary Change* 107: 59–69. <https://doi.org/10.1016/j.gloplacha.2013.04.007>
- Barry R (2008) Mountain weather and climate. 3rd edn. Cambridge University Press, New York
- Barry R, Gan TY (2011) The Global Cryosphere. Past, Present and Future. Cambridge University Press, New York
- Boeckli L, Brenning A, Gruber S, Noetzli J (2012) Permafrost distribution in the European Alps: calculation and evaluation of an index map and summary statistics. *The Cryosphere* 6: 807–820. <https://doi.org/10.5194/tc-6-807-2012>
- Chiarle M, Coviello V, Arattano M, Silvestri P, Nigrelli G (2015). High elevation rock falls and their climatic control: a case study in the Conca di Cervinia (NW Italian Alps). In *Engineering Geology for Society and Territory-Volume 1* (pp. 439-442). Springer, Cham. https://doi.org/10.1007/978-3-319-09300-0_84
- Chiarle M, Geertsema M, Mortara G, Clague J (2021) Relations between climate change and mass movement: Perspectives from the Canadian Cordillera and the European Alps. *Global and Planetary Change* 202: 103499 <https://doi.org/10.1016/j.gloplacha.2021.103499>
- Collins B, Stock G (2016) Rockfall triggering by cyclic thermal stressing of exfoliation fractures. *Nature Geoscience* 9: 395-400. <https://doi.org/10.1038/ngeo2686>
- Fischer L, Huggel C, Käab A, Haerberli W (2012a) Slope failures and erosion rates on a glacierized high-mountain face under climatic changes. *Earth Surface Processes and Landforms* 30: 836-846. <https://doi.org/10.1002/esp.3355>
- Fischer L, Purves RS, Huggel C, Noetzli J, Haerberli W (2012b) On the influence of topographic, geological and cryospheric factors on rock avalanches and rockfalls in high-mountain areas. *Natural Hazards and Earth System Science* 12: 241-254. <https://doi.org/10.5194/nhess-12-241-2012>
- French HM (2018) *The Periglacial Environment*. 4th edn. John Wiley & Sons Ltd, Chichester
- Gubler S, Fiddes J, Keller M, Gruber S (2011) Scale-dependent measurement and analysis of ground surface temperature variability in alpine terrain. *The Cryosphere* 5: 431-443. <https://doi.org/10.5194/tc-5-431-2011>
- Guerini M, Giardino M, Paranunzio R, Nigrelli G, Turconi L, Luino F., Chiarle M (2021) Slope failures at high elevation in the Italian Alps in the period 2000-2020. *Pangaea Data Publisher for Earth & Environmental Science*. <https://doi.pangaea.de/10.1594/PANGAEA.931824>
- Gruber S, Hoelzle M, Haerberli W (2004) Rock-wall temperatures in the Alps: modelling their topographic distribution and regional differences. *Permafrost and Periglacial Processes* 15: 299-307. <http://dx.doi.org/10.1002/ppp.501>
- Haberkorn A, Hoelzle M, Philips M, Kenner R (2015) Snow as a driving factor of rock surface temperatures in steep rough rock walls. *Cold Regions Science and Technology* 118: 64-75. <https://doi.org/10.1016/j.coldregions.2015.06.013>
- Haberkorn A, Phillips M, Kenner R, Rhyner H, Bavay M, Galos SP, Hoelze M (2016) Thermal regime of rock and its relation to snow cover in steep alpine rock walls: Gemsstock, central Swiss Alps. *Geografiska Annaler* 97 (3) 579-597. <https://doi.org/10.1111/geoa.12101>
- Harris C, Arenson L, Christiansen H, et al. (2009) Permafrost and climate in Europe: Monitoring and modelling thermal, geomorphological and geotechnical responses. *Earth Science Review* 92 (3-4): 117-171. <https://doi.org/10.1016/j.earscirev.2008.12.002>
- Hasler A, Gruber S, Haerberli W (2011) Temperature variability and offset in steep alpine rock and ice faces. *The Cryosphere* 5: 977-988. <https://doi.org/10.5194/tc-5-977-2011>
- Hock R, Rasul G, Adler C, Cáceres B, Gruber S, Hirabayashi Y, Jackson M, Käab A, Kang S, Kutuzov S, Milner A, Molau U, Morin S, Orlove B, Steltzer H (2019) High Mountain Areas. In: *IPCC Special Report on the Ocean and Cryosphere in a Changing Climate* [H.-O. Pörtner, D.C. Roberts, V. Masson-Delmotte, P. Zhai, M. Tignor, E. Poloczanska, K. Mintenbeck, A. Alegría, M. Nicolai, A. Okem, J. Petzold, B. Rama, N.M. Weyer (eds.)]. In press.
- Huggel, C, Clague JJ, Korup O (2012). Is climate change responsible for changing landslide activity in high mountains? *Earth Surface Processes and Landforms*, 37(1): 77-91. <https://doi.org/10.1002/esp.2223>
- Humlun O, Matsuoka N. eds. (2004) *A Handbook on Periglacial Field Methods*. International Permafrost Association. <https://ipa.arcticportal.org/publications/handbook> accessed 17 May 2018

- 1
2
3 Huwald H, Higgins CW, Boldi MO, Bou-Zeid E, Lehning M, Parlange MB (2009) Albedo effect on radiative errors
4 in air temperature measurements. *Water Resources Research* 45 (8): 1-13.
5 <https://doi.org/10.1029/2008WR007600>
- 6 Kellerer-Pirklbauer A (2017) Potential weathering by freeze-thaw action in alpine rocks in the
7 European Alps during a nine-year monitoring period. *Geomorphology* 296: 113-131
8 <https://doi.org/10.1016/j.geomorph.2017.08.020>
- 9 Knoflach B, Tussetschläger H, Sailer R, Meißl G, Stötter J (2021). High mountain rockfall dynamics: rockfall
10 activity and runout assessment under the aspect of a changing cryosphere. *Geografiska Annaler: Series A,*
11 *Physical Geography*, 103(1): 83-102. <https://doi.org/10.1080/04353676.2020.1864947>
- 12 Lucchesi S, Fioraso G, Bertotto S, Chiarle M (2014) Little Ice Age and contemporary glacier extent in the western
13 and south-western Piedmont Alps (north-western Italy). *Journal of Maps* 10 (3): 409-423.
14 <https://doi.org/10.1080/17445647.2014.880226>
- 15 Magnin F, Yosnin JY, Ravel L, Pergaud J, Pohl B, Deline P (2017) Modelling rock wall permafrost degradation
16 in the Mont Blanc massif from the LIA to the end of the 21st century. *The Cryosphere* 11 (4): 1813-1834.
17 <https://doi.org/10.5194/tc-11-1813-2017>
- 18 Matsuoka N, Murton J (2008) Frost Weathering: Recent Advances and Future Directions. *Permafrost and Periglacial*
19 *Processes* 19: 195-210. <https://doi.org/10.1002/ppp.620>
- 20 Merlone A, Lopardo G, Antonsen I, et al. (2012) A new challenge for meteorological measurements: the
21 “MeteoMet” project – metrology for meteorology. 9th International Symposium on Temperature. AIP Conf.
22 Proc. 1552, 1030-1035
- 23 Merlone A, Lopardo G, Sanna F, et al. (2015) The MeteoMet project - metrology for meteorology: challenges and
24 results. *Meteorological Applications* 22 (S1): 820–829. <http://dx.doi.org/10.1002/met.1528>
- 25 Ming-ko W (2015) *Permafrost Hydrology*. Springer-Verlag, Berlin Heidelberg
- 26 Moore J, Gischig V, Katterbach M, Loew S (2011) Air circulation in deep fractures and the temperature field of an
27 alpine rock slope. *Earth Surface Processes and Landforms* 36: 1985-1996. <http://dx.doi.org/10.1002/esp.2217>
- 28 Musacchio C, Coppa G, Merlone A (2018) An experimental method for evaluation of the snow albedo effect on
29 near-surface air temperature measurements. *Meteorological Application* 26 (1): 161-170.
30 <https://doi.org/10.1002/met.1756>
- 31 Nagai H, Fujita K, Nuimura T, et al. (2013) Southwest-facing slopes control the formation of debris-covered
32 glaciers in the Bhutan Himalaya. *The Cryosphere* 7: 1303-1314. <https://doi.org/10.5194/tc-7-1303-2013>
- 33 Nelson FE, Outcalt SI (1987) A computational method for prediction and regionalization of permafrost. *Arctic*
34 *and Alpine Research* 19 (3): 279-288. <https://doi.org/10.1080/00040851.1987.12002602>
- 35 Nigrelli G, Barbero S, Chiarle M (2021a) Solar radiation at the Bessanese high-elevation experimental site (Italy).
36 *Pangaea Data Publisher for Earth & Environmental Science*.
37 <https://doi.pangaea.de/10.1594/PANGAEA.930679>
- 38 Nigrelli G, Luino F, Turconi L, Guerini M, Paranunzio R, Giardino M, Chiarle M (2021b) Catasto delle frane di alta
39 quota nelle Alpi italiane. <http://geoclimalp.to.cnr.it/ILIA/index.html#6/45.019/9.382> Accessed on 23 June 2021
- 40 Nigrelli G, Fratianni S, Zampollo A, Turconi L, Chiarle M (2018) The altitudinal temperature lapse rates applied to
41 high elevation rockfalls studies in the Western European Alps. *Theoretical and Applied Climatology* 131: 1479-
42 1491. <https://doi.org/10.1007/s00704-017-2066-0>
- 43 Nigrelli G, Lucchesi S, Bertotto S, Fioraso G, Chiarle M (2015) Climate variability and Alpine glaciers evolution in
44 Northwestern Italy from the Little Ice Age to the 2010s. *Theoretical and Applied Climatology* 122 (3): 595-608.
45 <https://doi.org/10.1007/s00704-014-1313-x>
- 46 Paranunzio R, Chiarle M, Laio F, Nigrelli G, Turconi L, Luino F (2019a) New insights in the relation between
47 climate and slope failures at high-elevation sites. *Theoretical and Applied Climatology* 137: 1765-1784.
48 <https://doi.org/10.1007/s00704-018-2673-4>
- 49 Paranunzio R, Chiarle M, Laio F, Nigrelli G, Turconi L, Luino F (2019b) Slope failures in high-mountain areas in
50 the Alpine Region. *Pangaea Data Publisher for Earth & Environmental Science*.
51 <https://doi.pangaea.de/10.1594/PANGAEA.903761>
- 52 Paranunzio R, Laio F, Chiarle M, Nigrelli G, Guzzetti F (2016) Climate anomalies associated to the occurrence of
53 rockfalls at high-elevation in the Italian Alps. *Natural Hazards and Earth System Science* 16 (9): 2085–2106.
54 <https://doi.org/10.5194/nhess-16-2085-2016>
- 55 Ravel L, Magnin F, Deline P (2017) Impacts of the 2003 and 2015 summer heatwaves on permafrost-affected
56 rock-walls in the Mont Blanc massif. *Science of the Total Environment* 609: 132–143.
57 <https://doi.org/10.1016/j.scitotenv.2017.07.055>

- 1
2
3 Schnepfleitner H, Rode M, Sass O (2018) Validation of simulated temperature profiles at rock walls in the eastern
4 alps (Dachstein). *Permafrost and Periglacial Processes* 29: 34–48. <https://doi.org/10.1002/ppp.1962>
5 Schön JH (2015) *Physical Properties of Rocks*. 2nd edn. Amsterdam: Elsevier
6 Thorne PW, Diamond HJ, Godison S, et al. (2018) Towards a global land surface climate fiducial reference
7 measurements network. *International Journal of Climatology* 38: 2760–2774. <https://doi.org/10.1002/joc.5458>
8 van Everdingen RO ed. (1998) *Multi-language Glossary of Permafrost and related Ground-ice Terms*. *International*
9 *Permafrost Association*. Revised 2005
10 Viani C, Chiarle M, Paranunzio R, Merlone A, Musacchio C, Coppa G, Nigrelli G (2020) An integrated approach to
11 investigate climate-driven rockfall occurrence in high alpine slopes: the Bessanese glacial basin, Western
12 Italian Alps. *Journal of Mountain Science* 17: 2591–2610. <https://doi.org/10.1007/s11629-020-6216-y>
13 Weber S, Beutet J, Faillietaz J, et al. (2017) Quantifying irreversible movement in steep, fractured bedrock
14 permafrost on Matterhorn (CH). *The Cryosphere* 11: 567–583.
15
16
17
18
19
20
21
22
23
24
25
26
27
28
29
30
31
32
33
34
35
36
37
38
39
40
41
42
43
44
45
46
47
48
49
50
51
52
53
54
55

56 **Tables**

57
58
59
60

Table 1. Main characteristics of the three rock-faces (TMS No.) and the nine MT data logger (ID No.) used in this study. AGL, height of the hole in the rock, above the ground level. * also identified as near surface rock temperature (NSRT)

| TMS (No.) | Elevation (m a.s.l.) | Aspect (°N) | Slope (°) | Latitude (N) | Longitude (E) | ID (No.) | AGL (cm) | Depth (cm) |
|--------------|-------------------------|----------------|--------------|-----------------|------------------|-------------|-------------|---------------|
| TMS1 | 2667 | 30 | 50 | 45.29758 | 7.14259 | Q61213 | 100 | 10* |
| | | | | | | Q62122 | 100 | 30 |
| | | | | | | Q61215 | 100 | 50 |
| TMS2 | 2666 | 135 | 50 | 45.29702 | 7.14390 | Q61212 | 130 | 10* |
| | | | | | | Q62114 | 130 | 30 |
| | | | | | | Q62121 | 130 | 50 |
| TMS3 | 2653 | 225 | 45 | 45.29711 | 7.14421 | Q62110 | 100 | 10* |
| | | | | | | Q62097 | 100 | 30 |
| | | | | | | Q61211 | 100 | 50 |

Table 2. Measurement uncertainty components: D, Distribution; N, Normal; R, Rectangular; U, Uncertainty

| U component | Value (°C) | D | U (°C) |
|-----------------------------|---------------|---|-----------|
| U calibration | 0.027 | N | 0.027 |
| Resolution | 0.1 | R | 0.029 |
| Calibration curve residuals | Negl. | | 0.000 |
| Field comparability | 0.1 | R | 0.029 |
| Total U (K) | | | 0.049 |
| Total U (K=2) | | | 0.098 |

Table 3. Rock (ID No.) and air temperature (AWS) observed during the two years of measurements, from 20 July 2018 to 5 August 2020 (Tmean, Tmin and Tmax are respectively mean, minimum and maximum temperature; Sd, standard deviation; * data loggers that have acquired near surface rock temperature)

| ID (No.) | Tmean (°C) | Tmin (°C) | Tmax (°C) | Data (No.) | Sd (°C) |
|-------------|---------------|--------------|--------------|---------------|------------|
| Q61213* | 3.1 | -7.5 | 27.2 | 35858 | 5.4 |
| Q62122 | 3.0 | -5.7 | 20.7 | 35858 | 5.4 |
| Q61215 | 2.9 | -4.3 | 17.2 | 35858 | 5.0 |
| Q61212* | 5.4 | -2.7 | 33.0 | 35858 | 7.4 |
| Q62114 | 5.2 | -1.6 | 23.4 | 35858 | 6.4 |
| Q62121 | 5.1 | -1.8 | 20.5 | 35858 | 6.2 |

| | | | | | |
|---------|-----|-------|------|-------|-----|
| Q62110* | 5.6 | -5.0 | 40.8 | 35858 | 7.9 |
| Q62097 | 5.5 | -2.8 | 26.0 | 35858 | 6.2 |
| Q61211 | 5.5 | -1.8 | 20.5 | 35858 | 5.7 |
| AWS | 1.7 | -18.8 | 19.9 | 35158 | 6.7 |

Figure captions

Figure 1 Map of the Bessanese high-elevation experimental site. TMS, temperature monitoring site; AWS, Automatic Weather Station (owner ARPA Piemonte); Webcam, on the right glacial moraine at 2775 m a.s.l. (<https://bessanese.panomax.com/>); Black arrows indicates the glacier terminus at specific years (Aerial photo by Franco Rogliardo, 7 September 2016, source Comitato Glaciologico Italiano)

Figure 2 Drilling operations at TMS1 (A) and insertion of the temperature data logger at 30 cm depth (B)

Figure 3 Rock temperature trend at different depths (10 cm, 30 cm and 50 cm) at the three rock-faces (TMS1, TMS2 and TMS3) and air temperature and snow depth trends (AWS) acquired during the entire observation period. The different aspect of the measuring sites is also indicated (black circle in the wind rose)

Figure 4 Trend of rock temperature at TMS3 at the three different depths (10, 30, 50 cm), and of air temperature (Tair), during four consecutive days of September 2019 (1-2 September, cloudy days; 3-4 September, sunny days) in relation to the global (Gsr) and reflected (Rsr) solar radiation. Weather conditions of these four days can be checked by consulting the image archive of the webcam positioned to monitor the Bessanese experimental basin, at an altitude of 2775 m a.s.l. (<https://bessanese.panomax.com/>)

Figure 5 Descriptive statistics of the daily temperature lapse rate (DTLR, °C/cm) calculated in TMS1, TMS2 and TMS3, considering the two different depths intervals: a, 10 cm vs 30 cm; b, 30 cm vs 50 cm. In each box, the median and the mean are marked (respectively horizontal line and cross), the box edge indicate the first quartile (bottom) and the third quartile (top), the whiskers indicate the minimum (bottom) and the maximum (top) value

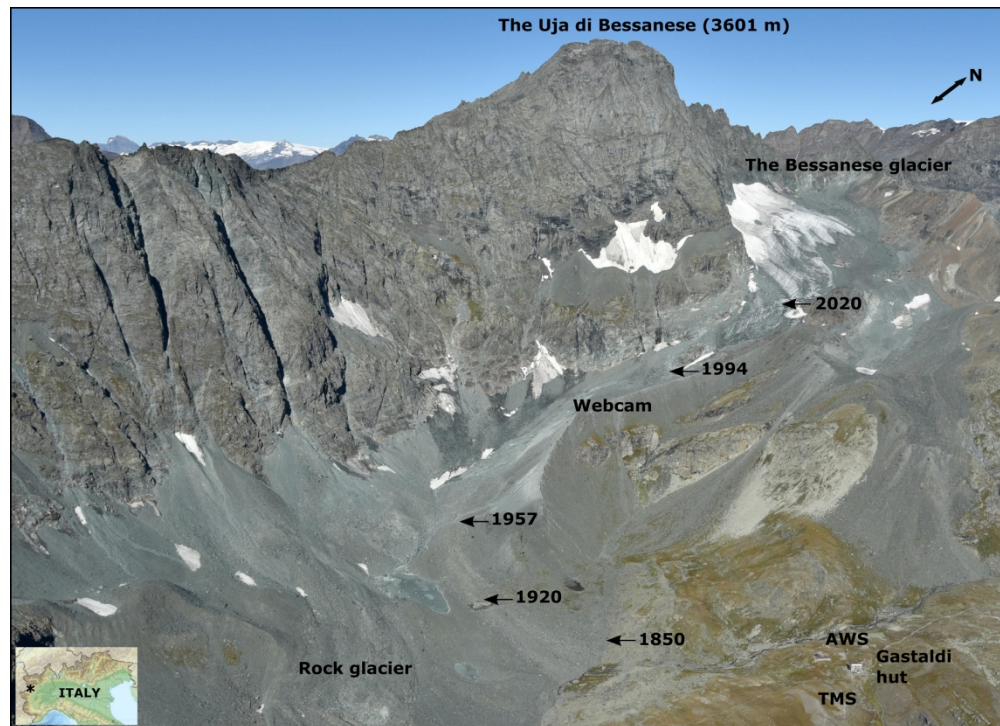


Figure 1 Map of the Bessanese high-elevation experimental site. TMS, temperature monitoring site; AWS, Automatic Weather Station (owner ARPA Piemonte); Webcam, on the right glacial moraine at 2775 m a.s.l. (<https://bessanese.panomax.com/>); Black arrows indicates the glacier terminus at specific years (Aerial photo by Franco Rogliardo, 7 September 2016, source Comitato Glaciologico Italiano)

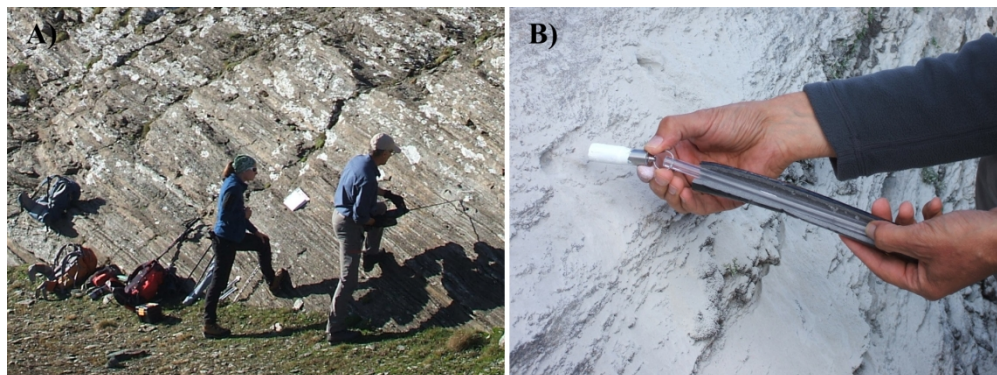


Figure 2 Drilling operations at TMS1 (A) and insertion of the temperature data logger at 30 cm depth (B)

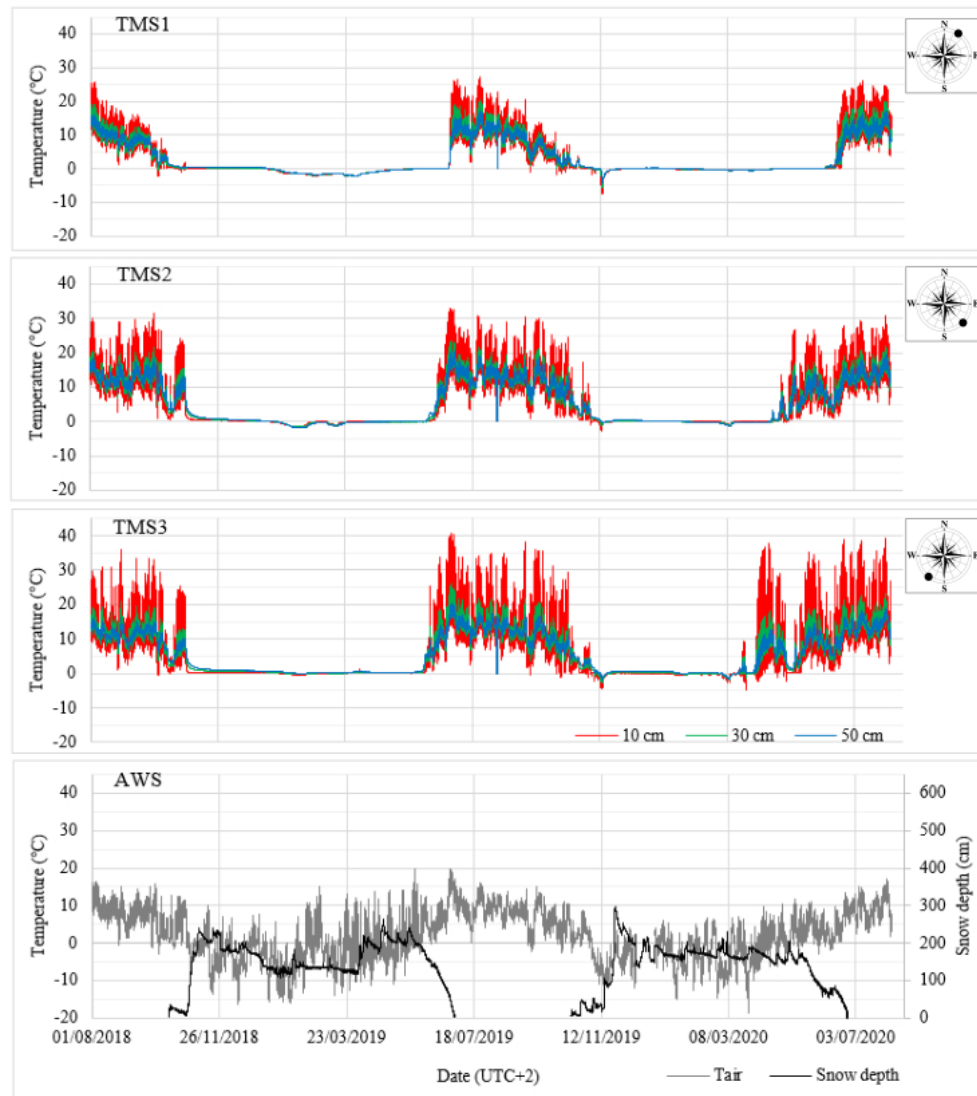


Figure 3 Rock temperature trend at different depths (10 cm, 30 cm and 50 cm) at the three rock-faces (TMS1, TMS2 and TMS3) and air temperature and snow depth trends (AWS) acquired during the entire observation period. The different aspect of the measuring sites is also indicated (black circle in the wind rose)

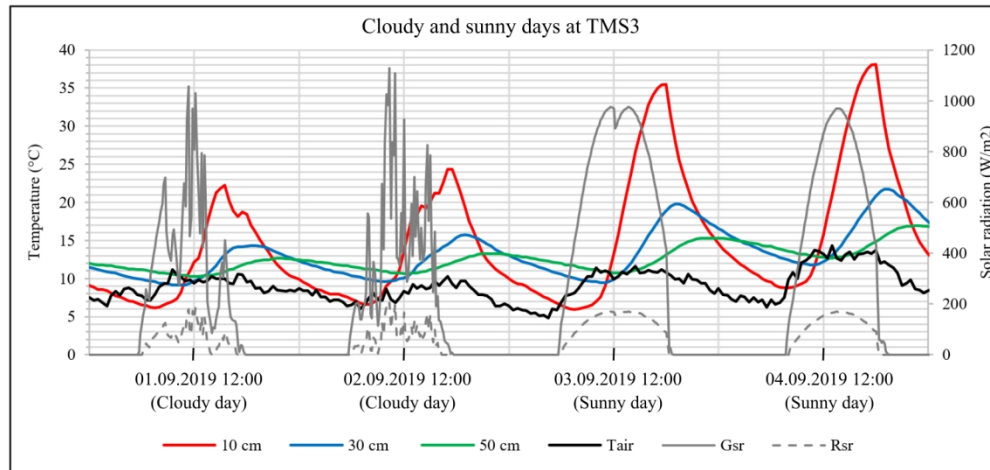


Figure 4 Trend of rock temperature at TMS3 at the three different depths (10, 30, 50 cm), and of air temperature (Tair), during four consecutive days of September 2019 (1-2 September, cloudy days; 3-4 September, sunny days) in relation to the global (Gsr) and reflected (Rsr) solar radiation. Weather conditions of these four days can be checked by consulting the image archive of the webcam positioned to monitor the Bessanese experimental basin, at an altitude of 2775 m a.s.l. (<https://bessanese.panomax.com/>)

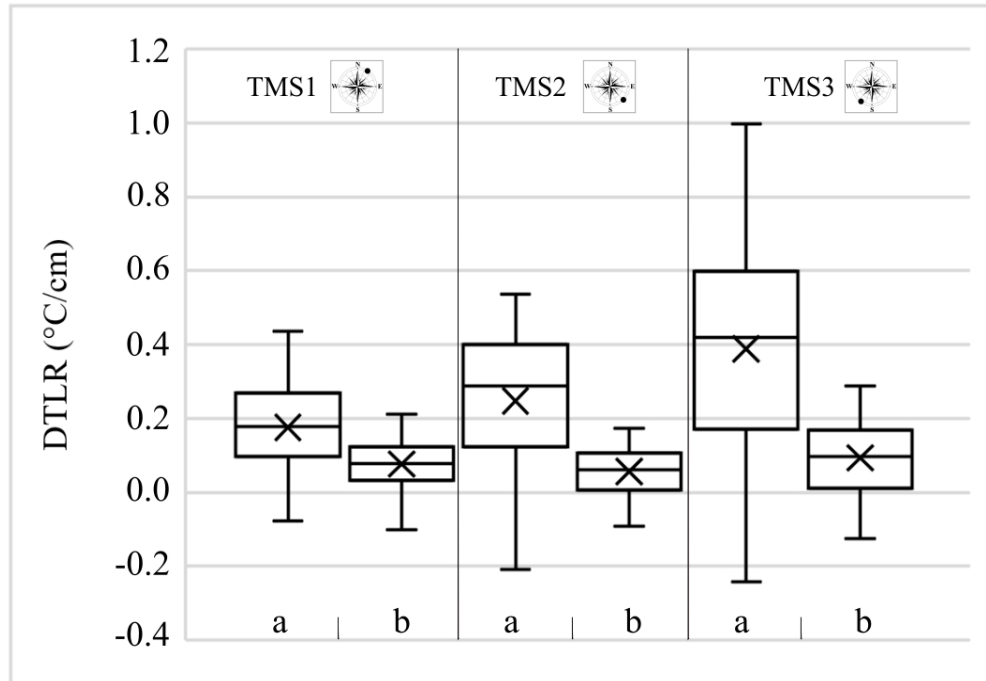


Figure 5 Descriptive statistics of the daily temperature lapse rate (DTLR, °C/cm) calculated in TMS1, TMS2 and TMS3, considering the two different depths intervals: a, 10 cm vs 30 cm; b, 30 cm vs 50 cm. In each box, the median and the mean are marked (respectively horizontal line and cross), the box edge indicate the first quartile (bottom) and the third quartile (top), the whiskers indicate the minimum (bottom) and the maximum (top) value